

# GIS-Driven Method for Site Feasibility Assessment of Large-Scale Solar Thermal Seawater Desalination: An Australian Case Study

Yingfei Huang<sup>1</sup>, Amr Omar<sup>1</sup>, David Saldivia<sup>1</sup>, Robert A. Taylor<sup>1</sup>, and Greg Leslie<sup>1,\*</sup>

<sup>1</sup> University of New South Wales, Australia

\* Correspondence: Greg Leslie, [g.leslie@unsw.edu.au](mailto:g.leslie@unsw.edu.au)

**Abstract.** Concentrated solar power (CSP) plants can be coupled with seawater desalination via Multi-Effect Distillation (MED) by recovering the cycle's 'free' waste heat. However, project viability, based on the payback period, is contingent upon systematic consideration of climate variability, topography, water resources, markets, and natural hazards. This study describes a data-driven method for screening and then selecting optimal sites in Australia by integrating a Geographic Information System (GIS), System Advisor Model (SAM), MATLAB program, and a Multi-Criteria Decision-Making (MCDM) model. Results for potential sites based on only climate, topography, water resources, markets, and infrastructure identify approximately  $2.13 \times 10^5$  km<sup>2</sup> of land are suitable, granularly mainly located in the north-west and the south coastal regions with high solar resources (average direct normal irradiance (DNI) > 6 kWh/m<sup>2</sup>day). These regions encompass 56,000 km<sup>2</sup> and 25,100 km<sup>2</sup> of suitable areas, respectively, with potential payback periods as low as 12.2 years and 14.0 years. Queensland's northern coastal regions also show promise with a potential payback period of 13.4 years, but the suitable area is only 2,070 km<sup>2</sup> due to the marine protection areas in the eastern coastal zone. New South Wales faces hurdles due to topography and lower solar resources. Model results were consistent with the development of CSP installations in Australia, particularly, the Aurora facility in South Australia. This study provides a precise delineation of CSP-MED integration regions in Australia through the multi-dimensional analysis, offering insights into payback periods, and quantifying variable impacts on project geographical, technical, and economic feasibility.

**Keywords:** Concentrated Solar Power, Multi-Effect Distillation, Geographical Information System, Techno-Economic Analysis, Site Selection

## 1. Introduction

Concentrated solar power (CSP) plants offer advantages over other renewable energy systems, including economies of scale, thermal storage capacity, and the opportunity to utilize waste heat for combined electricity and water cogeneration. Water and energy are intricately linked in CSP plants, where pure water is required for wet cooling and for cleaning reflectors to mitigate the impact of dust deposition on the heliostat's efficiency (the water usage for wet cooling is 15 times greater than that for mirror cleaning) [1]. It's estimated that cleaning 0.6 litres of freshwater per m<sup>2</sup> of concentrators incurs an additional cost of \$0.2 per square meter annually [2]. Combining a desalination unit within CSP plants designed to produce this water can eliminate or reduce this extra cost. However, selecting suitable sites to ensure the project's

financial feasibility is complex due to considering conflicting factors, including the availability of solar and water resources, topography, location of the residential area, constraints on land use, and natural disaster risks. These challenges indicate that a method to decide on feasible sites based on climate and market conditions is necessary.

Although several site selection efforts have employed GIS and the Multi-Criteria Decision-Making (MCDM) method, there has been a lack of comparative techno-economic feasibility analysis of the selected sites [3]. The existing literature primarily focuses on the siting of solar power plants instead of a hybrid solar desalination plant [3], which requires a deeper analysis including parameters such as seawater salinity, distance to the coastline, and land elevation.

In the previous work, the authors conducted a preliminary Geographical Information System (GIS)-based site selection and sensitivity analysis for key variables of several selected sites in Australia [4, 5]. The present study aims to extend this approach to evaluate the feasibility of a hybrid CSP and multi-effect distillation (MED) plant in Australia. [6].

This study uses a proposed method that incorporates a System Advisor Model (SAM) for CSP plant modelling, an in-house MATLAB techno-economic model for integrated CSP-MED system modelling, a GIS technique to screen the available area and an MCDM technique with an Analytical Hierarchy Process (AHP) for determining the factor weight to identify the best CSP-MED site in Australia. The factors include climate, topography, water resources, markets, land use, and natural hazards.

## 2. Methods

The detailed method is shown in the flow diagram of Figure 1. Input data (~20) are utilised in the site screening tool on a 10km × 10km grided (high resolution) map of Australia.

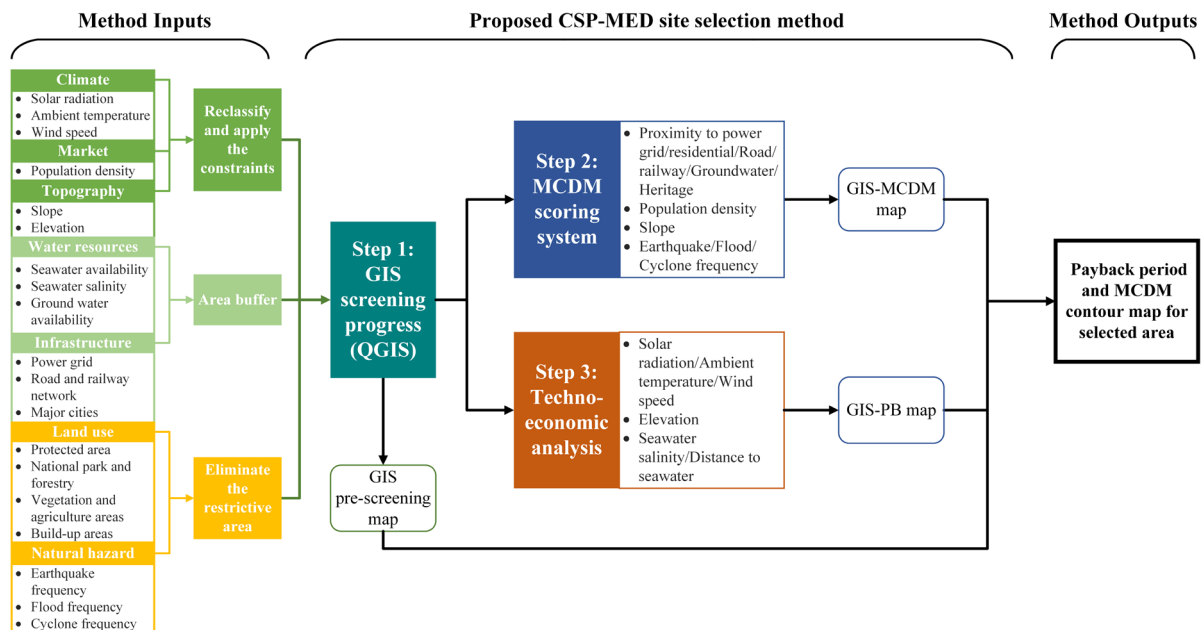


Figure 1. Flow diagram for proposed CSP-MED site selection method

The first stage involved applying constraints to the variables using GIS to carry out an initial screening, (e.g., urban areas, forests, and mountainous regions [7]). In addition, these cogeneration plants should be near infrastructure for efficient material transportation, electricity grid, distance to the coastline, and power stations. Also, these sites should not be prone to natural disasters, such as earthquakes, hurricanes, and floods. All of the above constraint layers are summarised in Table 1.

**Table 1.** Constraints and related justification for each parameter in the GIS screening process [8-12]

Layer	Feasibility Constraint Applied
Climate	Ensure the area with DNI>5 kwh/m <sup>2</sup> /day
Topography	Avoid high-slope areas and high-elevation areas
Nature hazard	Avoid flood, earthquake, and cyclone-prone areas
Land use	Avoid agriculture, urban, and heritage areas Proximity to the power grid, roads and railways, groundwater

The Quantum Geographic Information System (QGIS), was selected as the GIS screening tool. The variables considered in QGIS are global solar radiation, ambient temperature, wind speed, slope, elevation, population density, accessibility, hydrology, land availability, and seawater salinity. These variables and their descriptions are summarised in Table 2 and the GIS pre-screening map is illustrated in Figure 2.

**Table 2.** Inputs used in QGIS

Inputs	Geographical tool	Descriptions
DNI, ambient temperature, wind speed, Slope, elevation, population density, seawater availability	Zonal statistics	Statistics (mean and standard deviation) calculated from the values of raster cells falling within zones defined by the grid
Earthquake frequency	Count points in the polygon	Count the point number in the zones defined by the grid
Distance to the power grid (line), road and railways (points), groundwater (points), residential (points), heritage area (points)	Distance to the nearest hub (line to hub or points)	Indicate the distance to the nearest line vector or point vector
Agriculture area, build-up area, cyclone risk area, flood hazard area	Joins	Load the reclassified data to create the map and eliminate the unsuitable areas

Following this, the regions were assessed using the MCDM method and assigned a score with the weight factor of each variable determined by the AHP method [13-15]. This step was crucial in defining and optimizing the comparison of variables that could not be quantified through techno-economic analysis. Suitability scores are assigned to the selected variables under investigation according to the references [7-12, 16-20].

The remaining variables, namely direct normal irradiance (DNI), ambient temperature, wind speed, distance to seawater, elevation, and seawater salinity and seawater temperature, were subjected to analysis using a techno-economic model, with a focus on the payback period. The techno-economic model comprises two sections: the first section involves simulating the CSP plant using the System Advisor Model (SAM), while the second section incorporates the CSP-MED model in MATLAB code [21, 22]. Each subsystem, including the PTC, the Regenerative Feedwater Heating Rankine Cycle, and the cascaded MED system, is defined, and their interactions are modelled to evaluate system performance. Table 3 shows the design condition for the CSP-MED plant. This model was validated and published by the coauthors [19, 22].

**Table 3.** CSP-MED design conditions [21]

Input Parameters	Value	Input Parameters	Value
Net power output	50 MW	Solar multiple	2
High-pressure turbine inlet temperature	373°C	Thermal storage	8 hours
Low-pressure turbine inlet temperature	373°C	HTF hot temperature	391°C
Pumps isentropic efficiency	86%	HTF cold temperature	293°C
Turbine isentropic efficiency	85%		
Air cooler specific power (percentage of the net power generation)	5%	<b>MED design conditions</b>	
Closed feedwater heater effectiveness	80%	MED steam temperature	70°C
Low-pressure turbine splitting ratio	50%	Gain output ratio	10.36

Subsequently, the project's payback period, which concludes the levelized cost of water (LCOW) and electricity (LCOE) to calculate the number of years required to recover the project investment is used as the key indicator of this study. Suitable areas are determined by amalgamating the results obtained from the two abovementioned steps, ensuring that the MCDM score surpasses 40 points and the PB does not exceed 40 years. A 50 MWe CSP plant was determined according to most existing CSP plant capacity with an 8h thermal storage hour for nighttime operation.

The financial evaluation of the solar component in the CSP plant is derived from the financial model provided by the SAM software, specifically utilizing the calculation mode for the Power Purchase Agreement Single Owner of CSP Parabolic Trough projects. The costs associated with the pipes are determined through interpolation based on the plant's elevation and distance to the seawater. The economic model assumptions used are presented in Table 4.

**Table 4.** Economic model assumptions [23, 24]

Parameters	Symbol	Value
Plant availability	FC	96%
Operational period	n	25 years
Operating and maintenance-specific cost	$Z_{O\&M_{CSP}}$	66 \$/kWh·year
Real debt interest rate	$k_d$	6.5%
Annual insurance rate	$k_{ins}$	1%
Power purchase agreement	PPA	20 cents/kWh
Water purchase agreement	WPA	1.5 \$/m <sup>3</sup>

The total investment cost ( $Z_{inv}$ ), capital recovery factor ( $crf$ ), LCOE and LCOW are calculated using the following formulas:

$$Z_{inv} = Z_{inv} + Z_{inv} \quad (1)$$

$$crf = \frac{k_d(1 + k_d)^n}{(1 + k_d)^n - 1} + k_{ins} \quad (2)$$

$$LCOE = \frac{crf \times Z_{inv}(1 - E_p) + Z_{O\&M_{CSP}}}{Elec \times FC} \quad (3)$$

$$LCOW = \frac{crf \times Z_{inv}E_p + crf \times (Z_{MED} - Z_{Pipe}) + Z_{O\&M_{MED}}}{Dist \times FC} \quad (4)$$

$Elec$  and  $Dist$  represent the annual electricity generated (kWh/year) and the annual net water production (m<sup>3</sup>/year), respectively. It is important to highlight that  $Dist$  considers the water consumption of the CSP plant, which is relatively minor compared to the total water output of the MED system. This study assumes an equal market price for the water used for plant

operations and the water intended for sales.  $E_p$  denotes the percentage of electricity production allocated to operate the desalination plant. Finally, the payback period (PB) can be determined by considering power purchase agreements (PPA) and water purchase agreements (WPA) using the following formula:

$$PB = \frac{(LCOE \times Elec + LCOW \times Dist) \times n}{(PPA \times W + WPA \times Dist) \times FC} \quad (5)$$

### 3. Result and discussion

#### 3.1. GIS pre-screening result

After extracting the constraint layer, suitability recognition and mapping for CSP-MED sites in Australia were conducted, as illustrated in Figure 2. Then, the MCDM scoring, and the technical-economic analysis were applied to the preliminary screening results, respectively. The projection of the current or future CSP plant in Australia onto the map revealed that the preliminary GIS site selection method agreed with realistic CSP location choices in Western Australia, Queensland, and New South Wales.

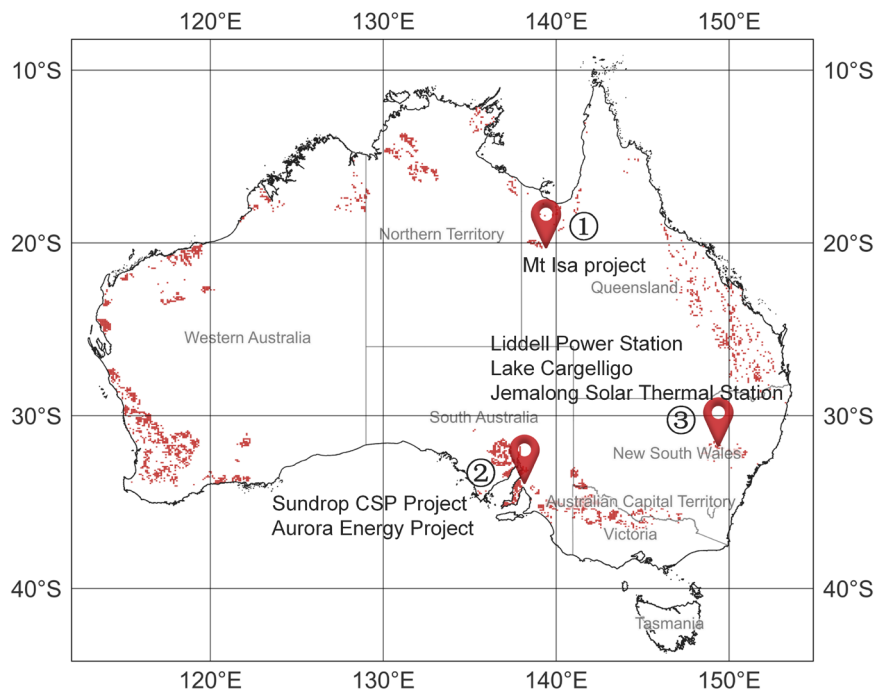


**Figure 2.** GIS pre-screening CSP-MED potential map with current and future CSP plants in Australia.

Following the initial screening and further analysis, the available land area for CSP-MED installation amounted to  $2.13 \times 10^5$  square kilometres, constituting 2.76% of the total national land area. Within the entire Australian territory, the MCDM scores for suitable regions, after removing areas scoring below 40 points, exhibited a mean value of approximately 54.7 points, while the average payback period amounted to 19.1 years. The highest MCDM score observed was 80.3 points and the minimum payback period is around 8.32 years. Figures 3 (a) and 3 (b) display the chosen region suitable for CSP-MED with categorized payback and MCDM scores.

Upon extracting the constraint layer on MCDM scores and payback periods, it is observed that areas, where current and future CSP plants are established in Queensland and

NSW regions, are not necessarily suitable for CSP-MED cogeneration plants. This is not surprising as stand-alone CSP plants are installed inland at sites with high solar resources, which tend to be far from the coastline. For example, the CSP plants in Mt Isa, Jemalong, and Sundrop CSP projects are 300 km, 350 km, and 12 km from the coastline, respectively. As such, this indicates that sites suitable for the CSP plant do not necessarily align with CSP-MED and it is important to conduct an integrated site feasibility assessment. Linking a MED process with Sundrop's CSP plant would decrease the payback period of the current plant by 37.5% from 16 years to 10 years.

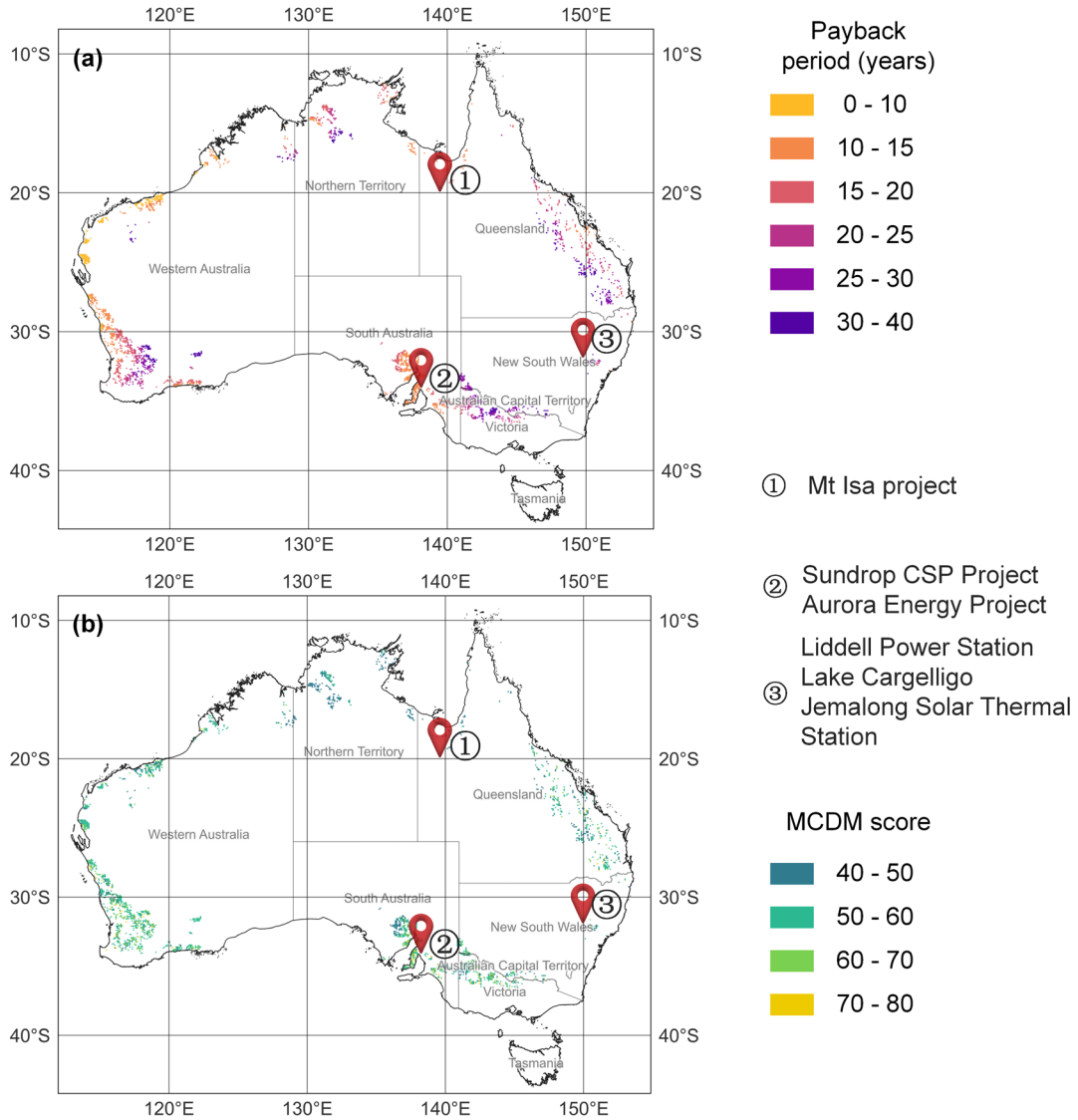


**Figure 3.** (a) Final MCDM score map (b) Final payback period map.

In terms of specific regions, Western Australia (WA) and South Australia (SA) exhibit higher feasibility for CSP-MED, with the Northern Territory (NT), Queensland (QLD), Victoria (VIC), and New South Wales (NSW) also displaying some suitable areas. However, the payback periods and the extent of suitable regions in Queensland and New South Wales are not ideal in comparison. Figure 4 and Figure 5 provide a zoomed-in representation with payback periods and MCDM scores of the predicted CSP-MED potential areas in Australia.

The DNI in Western Australia is notably favourable, with an average daily DNI of 6.75 kWh/m<sup>2</sup> in selected areas. The northern regions exhibit even higher values, with an average daily DNI of 7.57 kWh/m<sup>2</sup>, while the southern regions have a slightly lower average of 6.41 kWh/m<sup>2</sup>. This variance in DNI levels contributes to varying payback periods, with the northern

regions having an average payback period of 12.2 years, with a minimum of 8.32 years, and the southern regions having an overall average payback period of 19.3 years, with a minimum of 9.33 years. The total suitable area in Western Australia is approximately 56,000 km<sup>2</sup>, accounting for 26.3% of the total suitable land area. Notably, most suitable areas surround Perth in the southern part of Western Australia. The coastal areas of Western Australia have lower population densities compared to the eastern regions and are concentrated in a few major cities, such as Perth in the south, Geraldton in the west, and Karratha in the northwest. Although the majority of the northern regions of Western Australia has a very high DNI resources, limited access to electricity grids, a lack of infrastructure, and vulnerability to hurricanes, all reduce the extent of suitable land areas for CSP-MED.

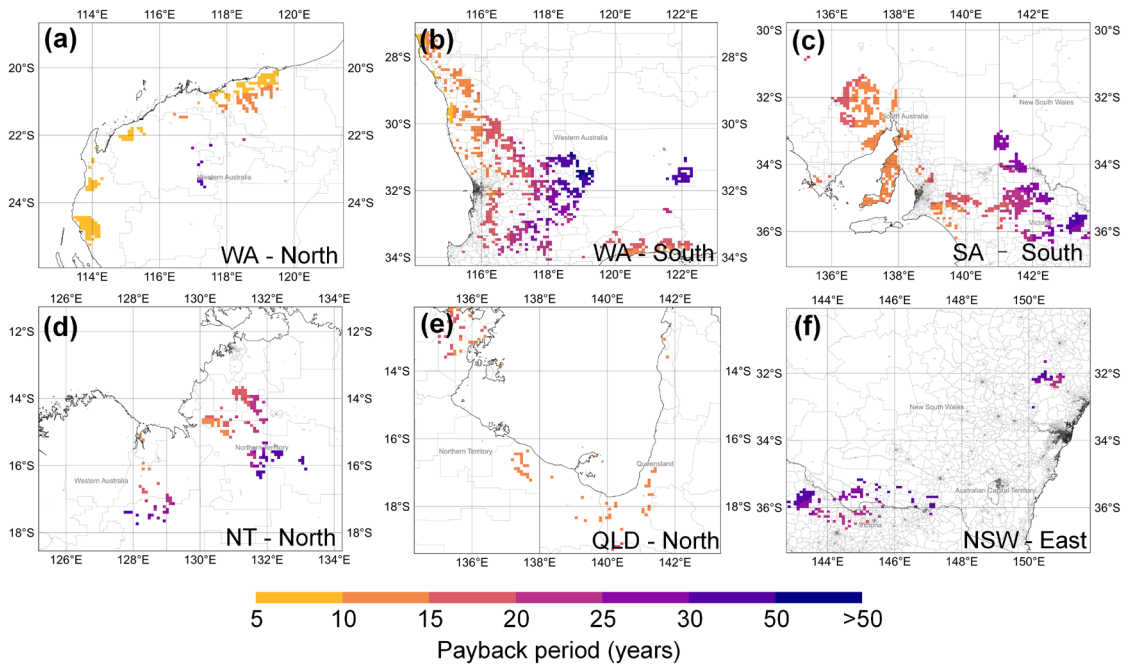


Figure 4. Zoomed-in payback period map for CSP-MED potential areas.

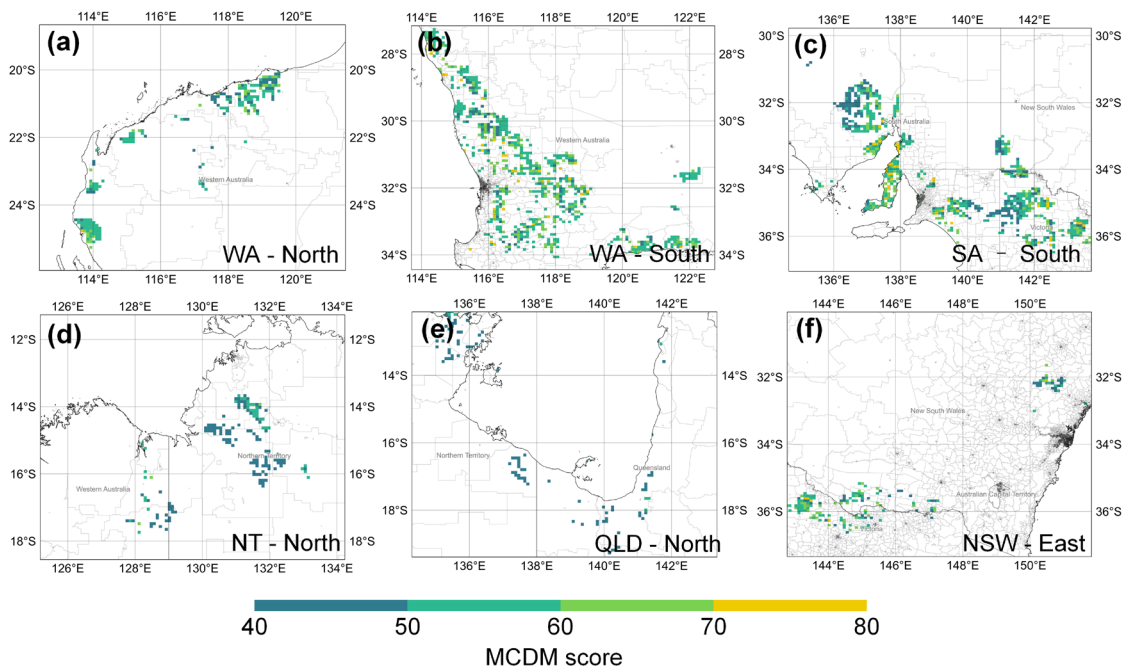


Figure 5. Zoomed-in MCDM score map for CSP-MED potential areas.

South Australia also demonstrates high feasibility for CSP-MED, with 25,100 km<sup>2</sup> of suitable land, primarily concentrated near Port Augusta. While the DNI in this region is lower compared to Western Australia, with an average daily DNI of 6.04 kWh/m<sup>2</sup>, it is still favourable. The payback period in this region is relatively favourable, with an average of 14.0 years and a minimum of 9.96 years. However, due to the DNI limitations, the minimum payback period is longer than that of Western Australia.

Queensland faces challenges due to its eastern coastal regions being unsuitable for CSP-MED due to their proximity to marine protection areas, particularly the Great Barrier Reef. Only certain coastal regions in the northern part of Queensland have been identified as partially suitable, covering an area of 2,070 km<sup>2</sup>. Despite having a smaller suitable area compared to other regions, Queensland has lower payback periods due to its favourable DNI (average daily DNI of 6.24 kWh/m<sup>2</sup>) and proximity to the coast. The average payback period in this region is 13.4 years.

The Northern Territory's suitable regions are in the coastal areas around Darwin, covering an area of 9,088 km<sup>2</sup>. However, the population is concentrated at a distance from the coast, and the electricity grid distribution is also distant from the coast, resulting in relatively average payback periods (average of 19.71 years) despite a relatively good daily DNI of 6.14 kWh/m<sup>2</sup>.

New South Wales exhibits the lowest suitability for CSP-MED, with only 6,390 km<sup>2</sup> of suitable land areas. The eastern coastal regions of NSW have the highest elevations in Australia and a significant mountain range, resulting in higher pumping and pipeline infrastructure costs. Additionally, the average daily DNI in this region is lower, at 5.97 kWh/m<sup>2</sup>. These factors contribute to an average payback period of 27.90 years for most areas in NSW. In Victoria, the challenge lies in insufficient solar resources, resulting in lower CSP efficiency. Most areas in Victoria have significantly higher payback periods.

MCDM scores for each region are displayed in the figures, with Western Australia and South Australia having average scores of 57.64 points and 56.10 points, respectively. These regions exhibit favourable payback periods and show high feasibility when considering other parameters, including population, topography, infrastructure, and natural hazards. Queensland and the Northern Territory yield more moderate MCDM scores, with averages of 40.4 points and 45.1 points, respectively. This is due to the relatively average distribution of population and infrastructure in these regions. It is noteworthy that New South Wales receives an average MCDM score of 54.2 points, indicating suitability for CSP-MED plant establishment from a conventional perspective. However, when factoring in the payback period, it becomes evident that most New South Wales sites are unsuitable for CSP-MED technology. In such cases, combining photovoltaic (PV) and RO might be a more suitable alternative, especially when considering solar-powered water desalination.

## 4. Conclusion

This study evaluated the feasibility of implementing CSP-MED plants in Australia. It employed a comprehensive geographical approach, including GIS screening, MCDM techniques, and an in-house techno-economic MATLAB model, to identify suitable sites. The results show that there is a  $2.13 \times 10^5$  km<sup>2</sup> suitable for CSP-MED installation in Australia. Across the entire country, the MCDM scores for viable areas, after eliminating those with scores below 40 points, averaged around 54.65 points, with an average payback period of approximately 19.08 years. Western Australia and South Australia emerged as highly feasible areas due to favourable solar conditions and infrastructure. Queensland showed potential in its northern coastal regions, while New South Wales faced challenges due to its mountainous terrain and lower solar resources. Simultaneously, the conclusion underscores the paramount significance of certain factors in influencing CSP-MED technology and its economic viability. According to the analysis, the current CSP plants are not suitable for CSP-MED except for the Sundrop CSP as it is near the coastline. These findings emphasize the importance of considering both

technical and economic factors when selecting CSP-MED plant locations, providing valuable insights for sustainable energy projects in Australia.

## Author contributions

**Yingfei Huang:** Conceptualization, Methodology, Software, Validation, Formal analysis, Investigation, Data Curation, Writing - Original Draft, Visualization. **Amr Omar:** Conceptualization, Methodology, Software, Validation, Writing - Review & Editing, Supervision. **David Saldivia:** Conceptualization, Methodology, Software, Validation, Writing - Review & Editing. **Robert A. Taylor:** Conceptualization, Writing - Review & Editing, Supervision, Project administration. **Greg Leslie:** Conceptualization, Writing - Review & Editing, Supervision, Project administration, Funding acquisition

## Competing interests

The authors declare that they have no competing interests.

## Data availability statement

The data supporting the findings of this article are derived from multiple sources and are available as follows:

Map	Spatial resolution	Data source	Map data and referenced databases
DNI	9 arc-sec (nominally 250 m)	Historical data (1994/1999/2007 to 2021)	Solargis [25]
Ambient temperature	30 arc-sec (nominally 1 km)	Historical data (1994-2021)	Solargis [25]
Wind speed	3 km	Historical data (1998-2017)	Global Wind Atlas 3.0 [26]
Population density	30 arc-sec (nominally 1 km)	Historical data (2020)	CIESIN [27]
Slope degree	30 m	Historical data (2023)	Ersi [28]
Elevation	30 arc-sec (nominally 1 km)	Historical data (2023)	Solargis [25]
Distance to seawater	0.01 degrees	Historical data (2009)	NASA OB.DAAC [29]
Seawater salinity	25 km	Historical data (2010-2019)	CEDA Archive [30]
Groundwater map, Land use, Build up area	10 m	Historical data (2017-2022)	Karra et al. [31]
Power grid	1 km	Derived map according to historical data (2020)	Predictive method [32]
Power station	-	Historical data (2018)	World Resources Institute [33]
Road and railway	30-500 m	Historical data (1980–2010)	CIESIN [34]
Protected area and heritage	at best 2 meters	Historical data (2023)	IUCN and UNEP-WCMC [35]
Earthquake frequency	-	Historical data (1970 to 2014)	OCHA [36]
Cyclone risk	at best 2 meters	1000 years return period based on historical data	UNISDR [37]
Flood risk potential	at best 2 meters	1000 years return period based on historical data	World Resources Institute [38]

These data are not publicly available due to third-party licensing restrictions. For further details on data access and use, please contact the corresponding author, Greg Leslie, at [g.leslie@unsw.edu.au](mailto:g.leslie@unsw.edu.au).

## References

- [1] T. Sarver, A. Al-Qaraghuli, and L. L. Kazmerski, 'A comprehensive review of the impact of dust on the use of solar energy: History, investigations, results, literature, and mitigation approaches', *Renewable and Sustainable Energy Reviews*, vol. 22, pp. 698–733, Jun. 2013, doi: 10.1016/j.rser.2012.12.065.
- [2] S. Bouaddi et al., 'A Review of Conventional and Innovative- Sustainable Methods for Cleaning Reflectors in Concentrating Solar Power Plants', *Sustainability*, vol. 10, no. 11, 2018, doi: 10.3390/su10113937.
- [3] L. Sun et al., 'A GIS-based multi-criteria decision-making method for the potential assessment and suitable sites selection of PV and CSP plants', *Resources, Conservation and Recycling*, vol. 168, 2021, doi: 10.1016/j.resconrec.2020.105306.
- [4] Y. Huang et al., 'Can Concentrated Solar Power + Desalination Solve Rising Energy and Water Prices? A n Australian Site Feasibility Study', in *Proceedings of the Asia Pacific Solar Research Conference 2022*, Australian PV Institute, Dec. 2022.
- [5] Y. Huang, A. Omar, D. Saldivia, R. A. Taylor, and G. Leslie, 'What Factors are Most Important in Determining Payback Period on Concentrated Solar Power+ Desalination Plants: A Sensitivity Analysis', in *Proceedings of the Asia Pacific Solar Research Conference 2022*, Australian PV Institute, Dec. 2022.
- [6] A. Omar, A. Nashed, Q. Li, G. Leslie, and R. A. Taylor, 'Pathways for integrated concentrated solar power - Desalination: A critical review', *Renewable and Sustainable Energy Reviews*, vol. 119, p. 109609, Mar. 2020, doi: 10.1016/j.rser.2019.109609.
- [7] L. Dawson and P. Schlyter, 'Less is more: Strategic scale site suitability for concentrated solar thermal power in Western Australia', *Energy Policy*, vol. 47, pp. 91–101, Aug. 2012, doi: 10.1016/j.enpol.2012.04.025.
- [8] A. Alami Merrouni, F. Elwali Elalaoui, A. Ghennioui, A. Mezrhab, and A. Mezrhab, 'A GIS-AHP combination for the sites assessment of large-scale CSP plants with dry and wet cooling systems. Case study: Eastern Morocco', *Solar Energy*, vol. 166, pp. 2–12, 2018, doi: 10.1016/j.solener.2018.03.038.
- [9] S. A. Mohamed, 'Application of geo-spatial Analytical Hierarchy Process and multi-criteria analysis for site suitability of the desalination solar stations in Egypt', *Journal of African Earth Sciences*, vol. 164, 2020, doi: 10.1016/j.jafrearsci.2020.103767.
- [10] A. Gerbo, K. V. Suryabagavan, and T. Kumar Raghuvanshi, 'GIS-based approach for modeling grid-connected solar power potential sites: a case study of East Shewa Zone, Ethiopia', *Geology, Ecology, and Landscapes*, vol. 6, no. 3, pp. 159–173, 2022, doi: 10.1080/24749508.2020.1809059.
- [11] A. Yushchenko, A. de Bono, B. Chatenoux, M. K. Patel, and N. Ray, 'GIS-based assessment of photovoltaic (PV) and concentrated solar power (CSP) generation potential in West Africa', *Renewable and Sustainable Energy Reviews*, vol. 81, pp. 2088–2103, 2018, doi: 10.1016/j.rser.2017.06.021.
- [12] A. T. A. Levosada, R. P. T. Ogena, J. R. V. Santos, and L. A. M. Danao, 'Mapping of Suitable Sites for Concentrated Solar Power Plants in the Philippines Using Geographic Information System and Analytic Hierarchy Process', *Sustainability (Switzerland)*, vol. 14, no. 19, 2022, doi: 10.3390/su141912260.
- [13] S. Ziuku, L. Seyitini, B. Mapurisa, D. Chikodzi, and K. van Kuijk, 'Potential of Concentrated Solar Power (CSP) in Zimbabwe', *Energy for Sustainable Development*, vol. 23, pp. 220–227, Dec. 2014, doi: 10.1016/j.esd.2014.07.006.
- [14] Y. Charabi and A. Gastli, 'PV site suitability analysis using GIS-based spatial fuzzy multi-criteria evaluation', *Renewable Energy*, vol. 36, no. 9, pp. 2554–2561, Sep. 2011, doi: 10.1016/j.renene.2010.10.037.
- [15] M. Uyan, 'GIS-based solar farms site selection using analytic hierarchy process (AHP) in Karapinar region, Konya/Turkey', *Renewable and Sustainable Energy Reviews*, vol. 28, pp. 11–17, Dec. 2013, doi: 10.1016/j.rser.2013.07.042.
- [16] O. S. Ohunakin and B. O. Saracoglu, 'A comparative study of selected multi-criteria decision-making methodologies for location selection of very large concentrated solar

- power plants in Nigeria', *African Journal of Science, Technology, Innovation and Development*, vol. 10, no. 5, pp. 551–567, 2018, doi: 10.1080/20421338.2018.1495305.
- [17] O. A. Omिताomu, N. Singh, and B. L. Bhaduri, 'Mapping suitability areas for concentrated solar power plants using remote sensing data', *Journal of Applied Remote Sensing*, vol. 9, no. 1, 2015, doi: 10.1117/1.JRS.9.097697.
- [18] 'Global model of cyclone wind 50, 100, 250, 500 and 1000 years return period - Humanitarian Data Exchange'. Accessed: May 23, 2023. [Online]. Available: <https://data.humdata.org/dataset/cyclone-wind-100-years-return-period>
- [19] A. Omar, D. Saldivia, Q. Li, R. Barraza, and R. A. Taylor, 'Techno-economic optimization of coupling a cascaded MED system to a CSP-sCO<sub>2</sub> power plant', *Energy Conversion and Management*, vol. 247, p. 114725, Nov. 2021, doi: 10.1016/j.enconman.2021.114725.
- [20] A. Gastli, Y. Charabi, and S. Zekri, 'GIS-based assessment of combined CSP electric power and seawater desalination plant for Duqum—Oman', *Renewable and Sustainable Energy Reviews*, vol. 14, no. 2, pp. 821–827, Feb. 2010, doi: 10.1016/j.rser.2009.08.020.
- [21] National Renewable Energy Laboratory, 'System Advisor Model (SAM 2020.11.29)'. Golden, CO, Dec. 27, 2020. [Online]. Available: <https://sam.nrel.gov>
- [22] D. Saldivia, C. Rosales, R. Barraza, and L. Cornejo, 'Computational analysis for a multi-effect distillation (MED) plant driven by solar energy in Chile', *Renewable Energy*, vol. 132, pp. 206–220, Mar. 2019, doi: 10.1016/j.renene.2018.07.139.
- [23] A. Omar, M. Saghafifar, and M. Gadalla, 'Thermo-economic analysis of air saturator integration in conventional combined power cycles', *Applied Thermal Engineering*, vol. 107, pp. 1104–1122, Aug. 2016, doi: 10.1016/j.applthermaleng.2016.06.181.
- [24] P. Palenzuela, D.-C. Alarcón-Padilla, and G. Zaragoza, 'Large-scale solar desalination by combination with CSP: Techno-economic analysis of different options for the Mediterranean Sea and the Arabian Gulf', *Desalination*, vol. 366, pp. 130–138, Jun. 2015, doi: 10.1016/j.desal.2014.12.037.
- [25] SOLARGIS, 'Solar resource maps and GIS map of World'. 2023. Accessed: Jun. 17, 2023. [Online]. Available: <https://solargis.com>
- [26] Global Wind Atlas 3.0, 'Worldwide mean wind speed at 10 m above surface level (m/s) - Global Wind Atlas'. Accessed: Jun. 17, 2023. [Online]. Available: <https://globalwindatlas.info>
- [27] Center for International Earth Science Information Network - CIESIN - Columbia University, 'Gridded Population of the World, Version 4 (GPWv4): Population Density, Revision 11'. NASA Socioeconomic Data and Applications Center (SEDAC), Palisades, New York, 2018. [Online]. Available: <https://doi.org/10.7927/H49C6VHW>
- [28] Esri, 'Terrain: Slope in Degrees'. Mar. 23, 2023. Accessed: Jun. 17, 2023. [Online]. Available: <https://www.arcgis.com/home/item.html?id=af25a795273440deb449b336543602be>
- [29] NASA Ocean Biology Processing Group, 'Distance to the Nearest Coast'. 2009. Accessed: Jun. 17, 2023. [Online]. Available: <https://oceancolor.gsfc.nasa.gov/docs/distfromcoast/>
- [30] J. Boutin et al., 'ESA Sea Surface Salinity Climate Change Initiative (Sea\_Surface\_Salinity\_cci): weekly and monthly sea surface salinity products, v03.21, for 2010 to 2020'. NERC EDS Centre for Environmental Data Analysis, 2021. doi: 10.5285/5920A2C77E3C45339477ACD31CE62C3C.
- [31] K. Karra, C. Kontgis, Z. Statman-Weil, J. C. Mazzariello, M. Mathis, and S. P. Brumby, 'Global land use / land cover with Sentinel 2 and deep learning', in 2021 IEEE International Geoscience and Remote Sensing Symposium IGARSS, Jul. 2021, pp. 4704–4707. doi: 10.1109/IGARSS47720.2021.9553499.
- [32] C. Arderne, C. Zorn, C. Nicolas, and E. E. Koks, 'Predictive mapping of the global power system using open data', *Sci Data*, vol. 7, no. 1, Art. no. 1, Jan. 2020, doi: 10.1038/s41597-019-0347-4.
- [33] Global Energy Observatory, Google, KTH Royal Institute of Technology in Stockholm, Enipedia, and World Resources Institute, 'Global Power Plant Database'. Resource Watch and Google Earth Engine, 2018. Accessed: Jun. 17, 2023. [Online]. Available: <http://resourcewatch.org/> <https://earthengine.google.com/>

- [34] Center For International Earth Science Information Network-CIESIN-Columbia University and Information Technology Outreach Services-ITOS-University Of Georgia, 'Global Roads Open Access Data Set, Version 1 (gROADSv1)'. Palisades, NY: NASA Socioeconomic Data and Applications Center (SEDAC), 2013. doi: 10.7927/H4VD6WCT.
- [35] IUCN and UNEP-WCMC, 'Protected Planet: The World Database on Protected Areas (WDPA)[On-line]'. Cambridge, UK, Jun. 2023. doi: <https://doi.org/10.34892/6fwd-af11>.
- [36] United Nations Office for the Coordination of Humanitarian Affairs (OCHA), 'Global catalog of earthquakes - Humanitarian Data Exchange'. Accessed: Jun. 17, 2023. [Online]. Available: <https://data.humdata.org/dataset/catalog-of-earthquakes1970-2014>
- [37] UN office for Disaster Risk Reduction (UNDRR), 'Global model of cyclone wind 50, 100, 250, 500 and 1000 years return period - Humanitarian Data Exchange'. Accessed: Jun. 17, 2023. [Online]. Available: <https://data.humdata.org/dataset/cyclone-wind-100-years-return-period>
- [38] World Resources Institute, 'Aqueduct Floods Hazard Maps'. Accessed: Jun. 17, 2023. [Online]. Available: <https://www.wri.org/data/aqueduct-floods-hazard-maps>